*High Pressure Research*
Vol. 00, No. 00, March 2009, 1–8

## RESEARCH ARTICLE

# *High-Resolution Neutron-Diffraction Measurements To 8 kbar*

C.L.Bull[a]*, A.D. Fortes[a], C.J. Ridley[a], I.G.Wood[b], D.P. Dobson[b], N.P.Funnell[a] A.S. Gibbs[a], C. Goodway[a], R. Sadykov[c] and K.S. Knight[b,d] [a]*ISIS Facility, Rutherford Appleton Laboratory, Chilton, OXON, OX11 0QX, UK.* [b]*Department of Earth Sciences, University College London, Gower Street, London WC1E 6BT, UK* [c]*Institute for Nuclear Research, Russian Academy of Sciences, pr. Shestidesyatiletiya Oktyabrya 7a, Moscow, 117312 Russia* [d]*Department of Earth Sciences, The Natural History Museum, Cromwell Road, London SW7 5BT UK.*

(*Received 00 Month 200x; in final form 00 Month 200x*)

We describe the capability to measure high-resolution neutron powder diffraction data to at least a pressure of 8 kbar. We have used the HRPD instrument at the ISIS neutron source and a piston-cylinder design of pressure cell machined from a null-scattering titanium zirconium alloy. Data were collected under hydrostatic conditions from an elpasolite perovskite $La_2NiMnO_6$; by virtue of a thinner cell wall on the incident-beam side of the cell, it was possible to obtain data in the instrument's highest resolution backscattering detector banks up to a maximum pressure of 8.5 kbar.

**Keywords:** neutron diffraction, high-pressure, perovskite, high-resolution

## 1. Introduction

Neutron diffraction provides unique and unparalleled insight into the position of light atoms in, for example, perovskite frameworks; the capabilities and advantages over other radiation sources for diffraction measurements has been well documented elsewhere, as have its applications when combined with high-pressure techniques [1–3]. On a time-of-flight (tof) neutron diffraction instrument the detectors remain fixed and the angle of the detector relative to the incident beam partially defines the instrument resolution. The resolution of a diffractometer, $\Delta d/d$ (where $\Delta d$ is the full width at half maximum height for a given Bragg peak), is a measure of the spread in uncertainty in the position of a Bragg reflection for a given d-spacing. The High Resolution Powder Diffractometer (HRPD) at ISIS is one of the highest resolution neutron powder diffractometers of its type in the world and is shown schematically in figure 1 [4]. The instrument is situated $\sim$ 100 m from the ISIS target and the neutrons are transported to the sample by a curved elliptical supermirror guide (the long flight path reduces the flight path uncertainty). In backscattering geometry (Figure 1) the $\Delta d/d$ resolution is $\sim 4\text{x}10^{-4}$. This resolution provides the ability to study subtle structural details and changes with temperature and pressure.

Traditionally, the pressures achievable on the HRPD instrument have been limited to that provided by gas cell technology $\sim$ 7 kbar [1], and unless the sample has

*Corresponding author. Email: Craig.Bull@stfc.ac.uk

ISSN: 0895-7959 print/ISSN 1477-2299 online

DOI: 10.1080/0895795YYxxxxxxxx
http://www.informaworld.com

high symmetry and is a good neutron scatterer, it is not of use for collecting data in the high-resolution backscattering detector bank. At the ISIS neutron source pressures beyond this range are provided by the McWhan pressure cell (up to $\sim$ 2.2 GPa) and the Paris Edinburgh press (up to $\sim$ 28 GPa) [5, 6]. However, these high-pressure devices are currently not suitable for use on the HRPD instrument as a result of the comparatively large beam divergence at the sample position. This is a result of the transport characteristics of the graded super-mirror guide [4], resulting in high backgrounds, and we are currently unable to use suitable beam collimation to solve this neutron issue without masking the high-resolution back scattering detectors.

In the current study we show how a high-pressure clamp cell (known as the HPC-11 pressure cell) can be used on the HRPD instrument to measure high-resolution data utilising the backscattering detector banks of the HRPD instrument up to 8.5 kbar with an applied load of 6 tonnes. The study has been performed on the monoclinic elpasolite perovskite $La_2NiMnO_6$ [7], which, at high pressure, is observed to transform to a rhombohedral structure.

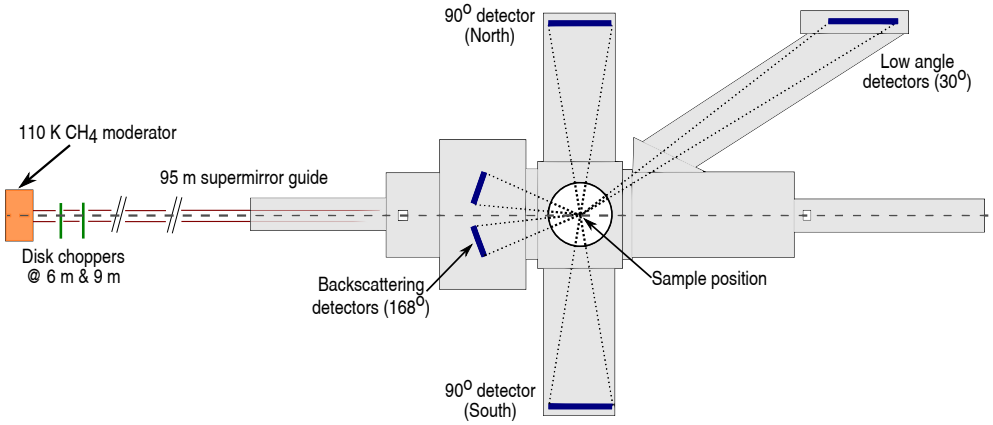


Figure 1. Schematic of the HRPD instrument. The incident beam is transported from the ISIS target through the methane moderator (at 110 K) from left to right. To avoid frame overlap a chopper system is employed prior to the curved (radius of curvature = 36 km), elliptical and graded (mostly M = 3) Ni-58 super-mirror guide which is 95 m in length. The neutrons arrive at the defined instrument centre where the sample is situated. Diffraction is measured using the three individual detector banks at 30° (low angle), 90° and 168°(high resolution). The HPC-11 pressure cell only permits simultaneous access to the 90° and 168° detector banks

## 2. The Pressure Cell Design

The HPC-11 pressure cell consists of two fretted cylinders, machined from an alloy of titanium and zirconium (TiZr) in the ratio of 67.7:32.3, with an external diameter of 36 mm, reduced to 25 mm in four window sections. The overall length of the assembled cell at high load is approximately 145 mm. This ratio Ti:Zr produces a null-scattering alloy which has high neutron transparency, with no Bragg reflections (the bound coherent scattering lengths of Ti and Zr are -3.44 and +7.16 fm respectively) [8]. However, it does show $Q$ $(4\pi\sin\theta/\lambda)$ dependent incoherent scattering. The hardness of the TiZr alloy is comparable to that of stainless steel. These neutronic and physical properties make it ideal for use as the body of a pressure clamp device suitable for neutron diffraction.

A schematic of the HPC-11 pressure cell is shown in Figure 2. The sample is loaded into polytetrafluoroethylene (PTFE) capsules with suitable pressure-transmitting media (PTM). The PTFE capsule is capped with a hard non-magnetic

alloy made of a nickel, chromium and aluminium containing alloy (known as 40HNU). The inner diameter of the inner bore of the TiZr body which the PTFE sits in is 8 mm, with an approximate sample diameter of 7.5 mm. Further pistons are inserted from both sides of the sample. Finally two further push rods are inserted from both ends. Load is applied to the clamp from two further push rods (not shown) driven from a suitable load frame and, to remove the loaded clamp from the frame, the load can be maintained by rotation of the hard aluminium alloy (V95T) nuts which hold the applied load without the loading frame. The clamp has been tested to 6 tonnes of applied load and generated 8 kbar of pressure at the sample position. It is also possible to make use of a suitable constant loading frame within the diffraction instrument, or to load the pre-pressurised clamp into a cryostat with a suitable internal bore. The minimum length of sample at maximum load is 15 mm.

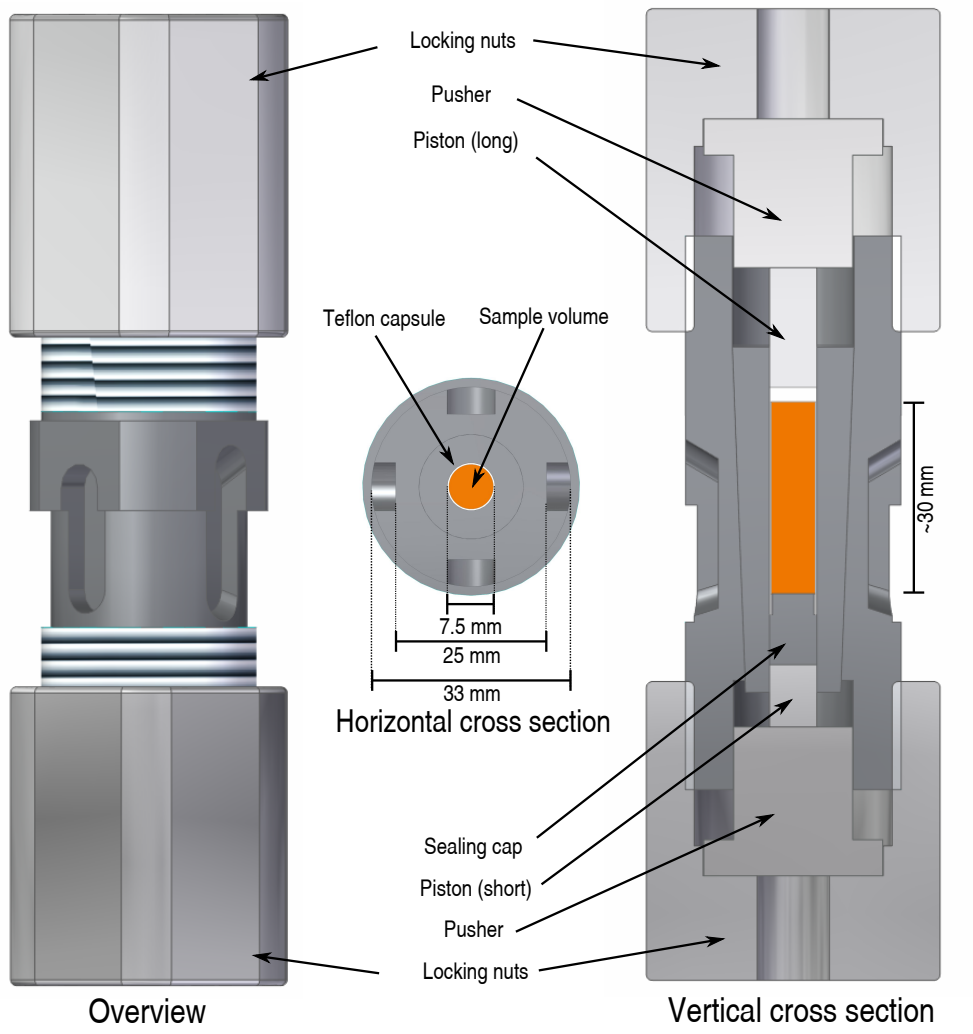


Figure 2. Left: Drawing of the assembled HPC-11 pressure cell. Right: Schematic of the HPC-11 assembly. Centre: Cross section at the beam height showing the four windows through which the incident and diffracted beams pass. Load is applied to the clamp via removable dies inserted into holes in the aluminium locking nuts.

## 3. Experimental

### 3.1. *Determination of load-pressure curves*

Powdered epsomite-d7 ($MgSO_4.7D_2O$), precipitated from a saturated aqueous solution of $MgSO_4$ in $D_2O$ during slow cooling was mixed with shavings of lead (to act as a pressure marker) in the mass ratio 1:0.6. These specimens were pressed by hand into the PTFE capsule of diameter 7.9 mm and length 25 mm, dampened with FC-77 fluorinert (to act as a pressure transmitting medium to maintain hydrostatic conditions), and then capped with a steel piston. The pressure-load curve for both cells was obtained using the engineering diffractometer, ENGIN-X, located at the ISIS Neutron Source in the UK. Time-of-flight diffraction data were collected from the sample within the bare PTFE pot mounted in order to obtain a zero-pressure/room-temperature dataset in the absence of pressure cell absorption. Subsequently, the PTFE capsule and dampened (with PTM) sample was inserted into the HPC-11 pressure cell, and the remaining steel piston elements were assembled, before mounting in the screw press installed on ENGIN-X to provide the load. Following the alignment of the cells, data were collected in the 20-60 ms time-of-flight window (25 Hz) with the specimen under no load for the purpose of quantifying the absorption by the cell. Thereafter, data were collected at applied loads of 1.5, 3.1, and 4.5 tonnes for the HPC-11 pressure cells. In order to determine the cell behaviour at low temperature, measurements were performed on the PEARL instrument [3] with the loaded pressure cell within a 100 mm bore Orange Helium cryostat at 6 tonnes and at temperatures of 290 and 120 K. Data was collected using the transverse detector banks. A sample of $La_2NiMnO_6$ was loaded along with NaCl as a pressure calibrant and fluorinert as a hydrostatic medium.

### 3.2. *High-resolution study of $La_2NiMnO_6$*

For the high-resolution study of the elpasolite perovskite, $La_2NiMnO_6$ was mixed with NaCl with a mass ratio of 3:1 (to act as a pressure calibrant) and 1:1 FC84 and FC87 fluorinert (to provide hydrostatic conditions). The cell was assembled as per the assembly shown in Figure 2 and placed in an Enerpac load frame. Load, in tonne increments, was applied and measured using a load cell. The assembled and loaded cell was then held on a standard 'candle stick' holder for the HRPD instrument (Figure 3). The height was adjusted and orientation for the incident beam marked using the specially designed alignment frame (Figure 3). A gadolinium mask was attached to the front face of the cell (through which the incident beam passes) in order to reduce cell scattering and ensure that only the sample volume was illuminated (Figure 3). The cell was then placed in the instrument and data collected in the 30-130 ms frame of the HRPD instrument providing a d-spacing range at 90° of $\sim$ 1–3.9 $\AA$ and at 168° (backscattering detectors) of $\sim$ 0.65–2.6 $\AA$. Data were collected for $\sim$ 8 hours per pressure point. After each data collection the cell was removed from the beam in order for the load to be increased; subsequently, masking foils were re-fitted and the cell was re-aligned for mounting on the beamline.

For all experiments, data were reduced using in-house software [10]. The final diffraction patterns were analysed using the GSAS suite [11]. The pressures were determined using the equation of state (EoS) of NaCl from Decker and for lead from the work of Fortes *et al* [12–14]. The sample pressure at low temperature was determined from the low temperature equation of state from the work of Skelton *et al* [9].

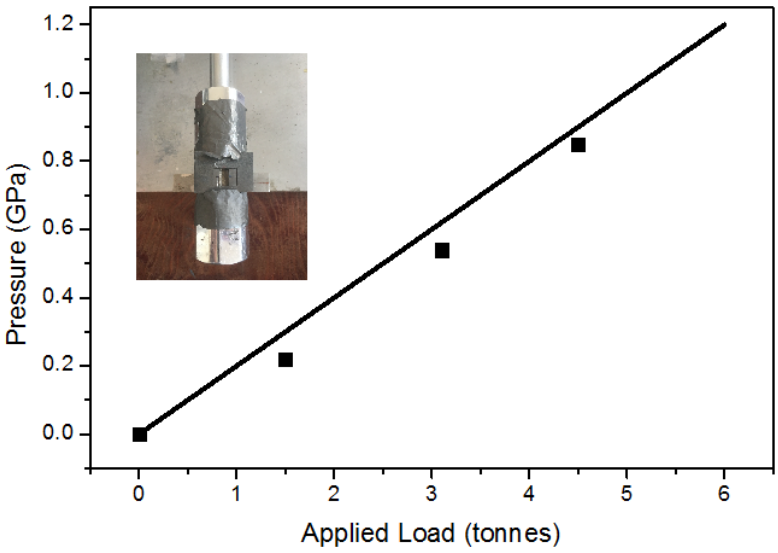


Figure 3. HPC-11 pressure cell with bespoke Gd foil incident and back-scattering beam shielding Pressure performance of the HPC-11 pressure cell, as a function of applied load from experiments performed on the ENGIN-X instrument. The pressure was measured from the known EoS of lead included in the sample container volume (see experimental and results for more information). The solid black line is the ideal pressure performance of the cell (neglecting any friction in the system). The insert shows the HPC-11 pressure cell with bespoke Gd foil incident and back-scattering beam shielding

## 4. Results & Discussion

### 4.1. *Pressure Cell Performance*

Figure 3 shows the pressure - load performance as determined from the ENGIN-X experiment for the HPC11 and pressure cell. The pressure was determined from the known EoS of lead [13, 14]. The maximum pressures achieved were 8 kbar for the HPC-11 pressure cell at the maximum working load. Once residual porosity was pressed out of the sample, the cell were pressurised at a rate of $\sim$ 2.1(1) kbar tonne$^{-1}$ which corresponds to the expected rate computed from the area of the piston (49.02 mm$^2$). As determined from the scale factors of the refined diffraction patterns (outwith and within the pressure cell), we found that the transmittance of HPC11 is $\sim$ 50 %. As a result of the diffracted beam collimation on the detectors of ENGIN-X, no background structure from the TiZr cell components was discernible, and parasitic scattering from the steel pistons only became apparent at high loads; the latter was eliminated by reducing the size of the incident beam by a set of jaws. Data was collected on the PEARL instrument at 6 tonnes applied load both at 290 and 120 K. At 290 K the pressure was determined to be 8.6(5) kbar and upon cooling to 120 K the pressure dropped to 5.0(5) kbar.

### 4.2. *A high-resolution study of $La_2NiMnO_6$ to 0.8 GPa*

The crystal structure of $La_2NiMnO_6$ has been well studied at ambient pressure and it has been shown to crystallise with monoclinic symmetry $P2_1/n$ [7]. However, this structure determination was only possible using high-resolution neutron diffraction; previous x-ray and lower resolution neutron studies had incorrectly reported it to be orthorhombic in symmetry. The monoclinic symmetry permits ordering of

the nickel and manganese on specific crystallographic Wyckoff sites ($2a$ and $2c$ respectively) and has been well described elsewhere [7]. At elevated temperatures the crystal symmetry transforms to rhombohedral, maintaining the B-site ordering with the space group $R\bar{3}$.

With the sample of $La_2NiMnO_6$, loaded with NaCl and fluorinert, diffraction data were obtained at ambient pressure and are shown in Figure 4. Data are shown from both the transverse and high-angle detector banks (90 and 168°). At ambient pressure the 202, 022 and $20\bar{2}$ reflections are observable for the monoclinic phase centred around 2.24 $\mathring{A}$ in the 90° bank; the 202 reflection is observable to lower d-spacing as a shoulder relative to the closely overlapping 022 and $20\bar{2}$ reflections. Upon going to the high-angle 168° detector bank it is possible to resolve the fitted peaks, demonstrating the power of the high resolution detector bank to enable the determination of subtle distortions in crystal symmetry. The full d-spacing range of data collected from both detectors at ambient pressure within the pressure cell are shown in the bottom part of Figure 4. Also shown is the background contribution from the empty pressure cell.

Figure 4 also shows the diffraction patterns up to pressures of 0.8 GPa. Upon increasing pressure, the relative intensity of the reflections centred around $\sim$2.24$\mathring{A}$, observed from data collected in the 90° detector banks, are seen to change: a shoulder at lower d-spacing decreases in intensity. Extra reflections are also seen to appear at d-spacings of $\sim$ 2.20 $\mathring{A}$. Upon indexing the new reflections at 0.8 GPa it can be shown that they are indexible on the the rhombohedral phase previously observed at high temperature at ambient pressure [7]. The new reflections are the 222 reflections around 2.2 $\mathring{A}$ reflections in the $R\bar{3}$ space group. The growing reflection at $\sim$ 2.29 $\mathring{A}$ is accountable by the anvils of the clamp itself. A full list of reflections in this region is given in Figure 4. The benefit of the 168° backscattering detector brings is clear in its ability to resolve the changes in diffraction pattern over that measured at 90°. The difference in the ability of the two detector banks to resolve the subtle changes in the diffraction pattern and hence determine the structural transition is clear. The poorer statistics in the backscattering 168° datasets is a result of the number of scattered neutrons satisfying the Bragg condition being inversely proportional to $\sin^2(\theta/2)$ and the difference in solid angle which is large. Data within the diffraction patterns allows us to follow the nature and extent of the phase transition with increasing pressure. Figure 5 shows the values of the lattice parameters determined by Le-Bail intensity extraction from the diffraction data as a function of pressure. There is only a small decrease in the determined lattice parameters which is understandable as the bulk modulus of $La_2NiMnO_6$ is estimated form data collected at higher pressure elsewhere to be 142(6) GPa and data collection is only possible over a small pressure range in the current experiment. However, what is clear from the diffraction pattern is the change from the monoclinic to rhomobohedral phase with increasing pressure.

## 5. Conclusions

We have demonstrated the capability to measure high-resolution neutron-diffraction data up to 8.4 kbar for the first time in back-scattering geometry, as a result of the unique geometry of the pressure cells. By making use of this pressure cell we have shown the transition of $La_2NiMnO_6$ elpasolite perovskite from the monoclinic phase to a high pressure rhombohedral phase (previously only observed at high temperature and ambient pressure). This work demonstrates the power of being able to obtain high-resolution neutron diffraction data at high pressure and

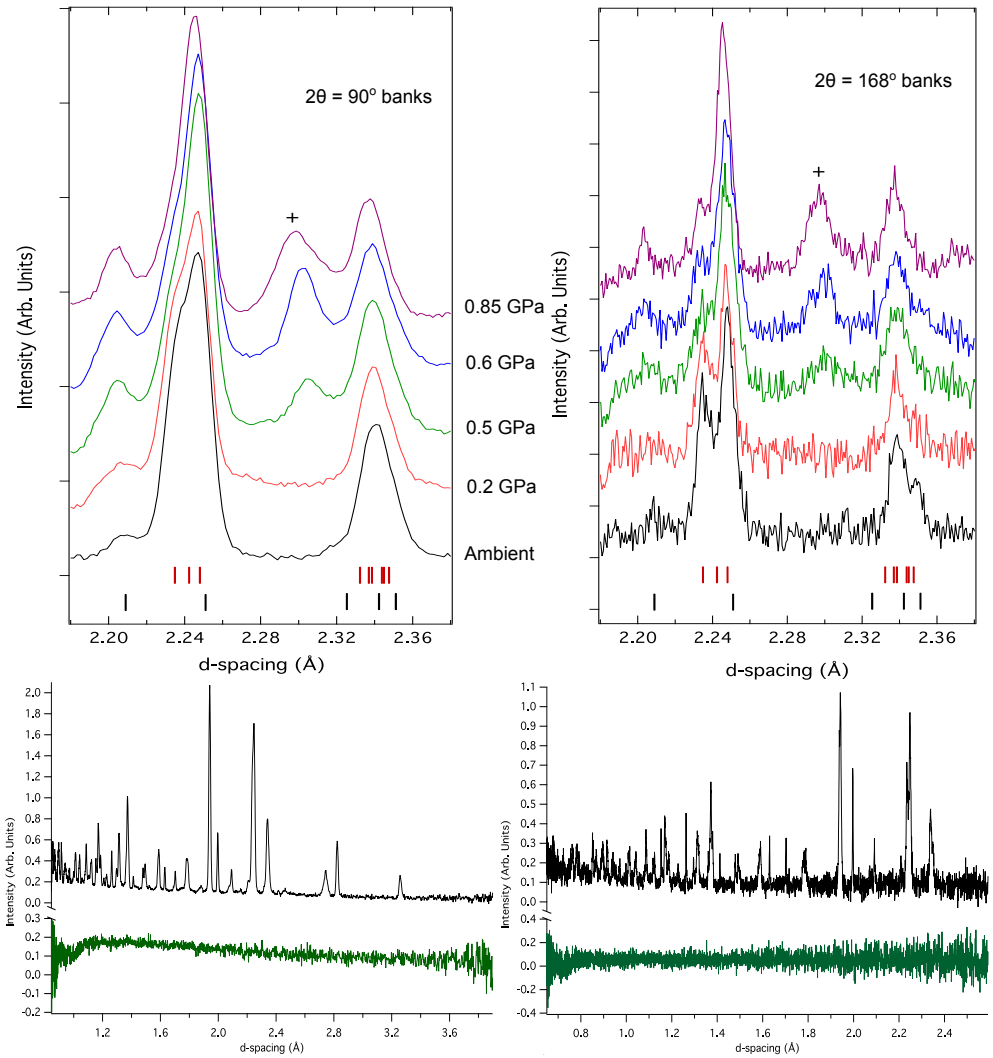


Figure 4. Top Left: Region of diffraction pattern of $La_2NiMnO_6$ measured on the 90° detector bank of HRPD as a function of pressure showing reflections where phase transition can be observed. Top Right: Same sample and d-spacing region with data measured using the 168° backscattering detector bank. The bottom of both diffraction patterns show the tick marks for each phase. The peak marked (+), seen to grow in intensity with pressure, is attributed to the piston material from the pressure cell. Top tick marks (vertical bars) indicate the expected positions for the 202, 20$\bar{2}$, 022, 211, 103, 21$\bar{1}$, 013, 10$\bar{3}$, 121 & 12$\bar{1}$ reflections (with increasing d-spacing respectively) of the monoclinic phase of $La_2NiMnO_6$ and the bottom tick marks the 222, 200, 122, 0$\bar{1}\bar{2}$/210 & 1$\bar{1}\bar{1}$ reflections (with increasing d-spacing) from the rhombohedral phase of $La_2NiMnO_6$. Bottom Left: Full diffraction pattern (30-130 ms frame) obtained from 90° detector bank of HRPD from $La_2NiMnO_6$ in HPC-11 at ambient pressure the bottom trace shows the diffraction pattern of the empty cell. Bottom Right: Full diffraction pattern (30-130 ms frame) obtained from 168° detector bank of HRPD from $La_2NiMnO_6$ in HPC-11 at ambient pressure the bottom trace shows the diffraction pattern of the empty cell.

will find applications in many crystalline systems on the HRPD instrument at ISIS and beyond.

## 6. Acknowledgements

This work was partly funded by the by the Science and Technology Facilities Council via grant PP/C501992/1, STFC consolidated grant number ST/K000934/1 and NERC grant NE/K002902/1. We acknowledge the ISIS cryogenic section for assistance with the cryostat experiment. The work was further supported through resources made available by the Science and Technology Facilities Council through the ISIS Neutron Facility.

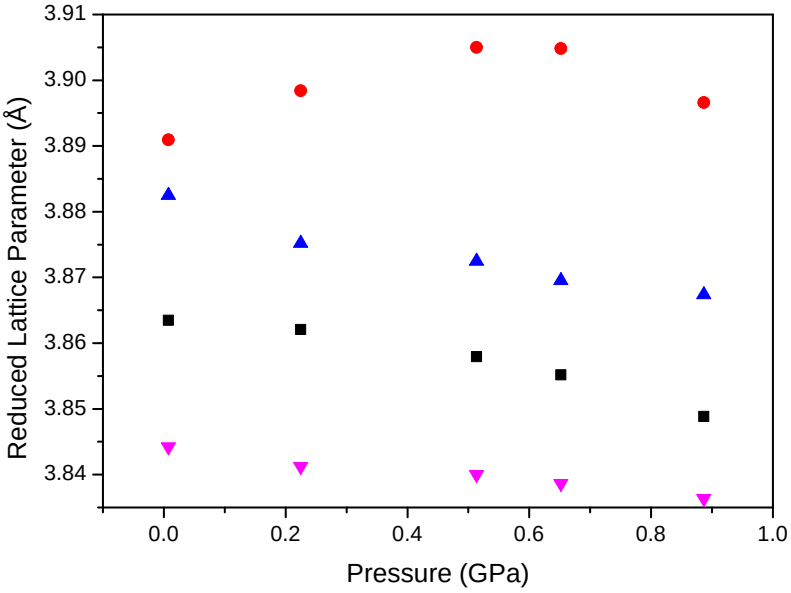


Figure 5. Determined lattice parameters as a function of pressure for both the monoclinic and rhombohedral unit cell of $La_2NiMnO_6$. Shown are the three equivalent lattice parameters ($a_{pc}$) for the cubic perovskite (where, for the orthorhombic lattice parameters, a = $\sqrt{2}a_{pc}$ (squares), b = $\sqrt{2}b_{pc}$ (circles) and c = $2c_{pc}$ (triangles) and for the rhombohedral unit cell =$\sqrt{2}a_{pc}$ (inverted triangle)).

## References

[1] S. Klotz *Techniques in High Pressure Neutron Scattering*, Taylor and Francis, Boca Raton, 2013.
[2] M. Guthrie, *Future directions in high-pressure neutron diffraction*, J. Phys.: Condens. Mat. 27 (2015), p. 153201.
[3] C. Bull, N. Funnell, M. Tucker, S. Hull, D. Francis, and W. Marshall, *PEARL: the high pressure neutron powder diffractometer at ISIS*, High Pressure Research 36 (2016), pp. 493–511.
[4] R.M. Ibberson, *Design and performance of the new supermirror guide on HRPD at ISIS*, Nuclear Instruments and Methods in Physics Research Section A: Accelerators, Spectrometers, Detectors and Associated Equipment 600 (2009), pp. 47 – 49.
[5] J.M. Besson, R.J. Nelmes, G. Hamel, J.S. Loveday, G. Weill, and S. Hull, *Neutron powder diffraction above 10 GPa*, Physica B 180 (1992), pp. 907–910.
[6] D.B. McWhan, D. Bloch, and G. Parisot, *Apparatus for neutron diffraction at high pressure*, Rev. Sci. Inst. 45 (1974), pp. 643–646.
[7] C.L. Bull, D. Gleeson, and K.S. Knight, *Determination of B-site ordering and structural transformations in the mixed transition metal perovskites La 2 CoMnO 6 and La 2 NiMnO 6*, Journal of Physics: Condensed Matter 15 (2003), p. 4927.
[8] V.F. Sears, *Neutron scattering lengths and cross sections*, Neutron News 3 (1992), pp. 26–37.
[9] E.F. Skelton, A.W. Webb, S.B. Qadri, S.A. Wolf, R.C. Lacoe, J.L. Feldman, W.T. Elam, E.R.C. Jr., and C.Y. Huang, *Energy-dispersive x-ray diffraction with synchrotron radiation at cryogenic temperatures*, Review of Scientific Instruments 55 (1984), pp. 849–855.
[10] O. Arnold et al., *Mantid—Data analysis and visualization package for neutron scattering and $\mu$SR experiments*, Nucl. Instrum. Meth. A 764 (2014), pp. 156–166.
[11] B.H. Toby, *EXPGUI, a graphical user interface for GSAS*, J. Appl. Crystallogr. 34 (2001), pp. 210–213.
[12] D.L. Decker, *Equation of state of sodium chloride*, J. Appl. Phys. 37 (1966), pp. 5012–5014.
[13] A.D. Fortes, I.G. Wood, M. Alfredsson, L. Voadlo, K.S. Knight, W.G. Marshall, M.G. Tucker, and F. Fernandez-Alonso, *The high-pressure phase diagram of ammonia dihydrate*, High Pressure Research 27 (2007), pp. 201–212.
[14] *Corrigendum*, High Pressure Research 32 (2012), pp. 337–337.